

IMPACT OF A PHOTOCATALYTIC OXIDATION LAYER COVERING THE INTERIOR SURFACES OF A REAL TEST ROOM: VOLATILE ORGANIC COMPOUND MINERALISATION, RISK ASSESSMENT OF BY-PRODUCT AND NANOPARTICLE EMISSIONS.

Franck Alessi*¹, Didier Therme¹

*1 CEA, INES, SBST, LGEB,
50 avenue du lac Léman (bâtiment HELIOS)
F-73377 Le Bourget-du-lac, France.
frank.alessi@cea.fr

ABSTRACT

Many studies about photocatalytic oxidation (PCO) have been carried out in laboratories. They use an inert test chamber with ideal indoor conditions: a low volume, a controlled temperature and humidity, and a constant injection of one to five specific gases. The principal aim of this study was to implement, in a real test room (TR) of an experimental house, a titanium dioxide (TiO₂) layer to quantify its efficiency. This layer, directly in contact with the indoor air (IA), was one of the four layers embedded in a passive system (PS) specifically designed to improve the indoor air quality (IAQ) and the thermal comfort. A specific monitoring in the TR assessed the removal rate of the volatile organic compounds (VOCs), as well as formaldehyde (HCHO) as a possible intermediate, and the nanoparticle (NP) emissions. In addition, a comparison was made with a reference room (RR) which was not equipped with the PS.

KEYWORDS

Photocatalytic oxidation, Indoor air quality, Volatile organic compounds, Nanoparticles, Real test room.

1 INTRODUCTION

The photocatalytic oxidation may be divided into six elemental mass transfer processes occurring in series (Zhong et al., 2010): 1) Advection (pollutants are carried by airflows), 2) External diffusion of reagent species through the boundary layer (BL) surrounding the catalyst or catalyst pellet, 3) Adsorption onto the catalyst surface, 4) Chemical reaction at the catalyst surface, 5) Desorption of reaction product(s), 6) Boundary layer diffusion of product(s) to the main airflow.

One of the most common choices of photocatalyst is titanium dioxide. This TiO₂ has two crystal forms: Anatase and Rutile with respectively an energy band-gap of 3.23eV and 3.02eV. When the TiO₂ semiconductor is illuminated by photons, an electron in an electron-filled valence band (VB) is excited by photoirradiation (the energy $h\nu$ must be equal or greater than the band-gap energy) toward a vacant conduction band (CB), leaving a positive hole in the VB (Mo et al., 2009). The key step in photocatalysis is the formation of hole-electron pairs on irradiation with UV-light. The energy of UVA [$320 \leq \lambda(nm) \leq 400$], UVB [280

$\leq \lambda(nm) \leq 320$], UVC [$100 \leq \lambda(nm) \leq 280$], are widely used because it is equal or greater than the 3.2eV band-gap energy of TiO₂ (Zhong et al., 2010).

These electrons and positive holes drive reduction and oxidation, respectively, of compounds adsorbed on the surface of a photocatalyst such as oxygen 'O₂', water vapor 'H₂O', 'VOCs' (Ginestet et al., 2005; Auvinen et al., 2008; Zhong et al., 2010; Mo et al., 2009).

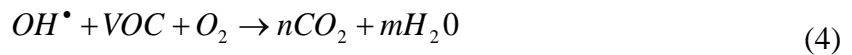
The activation equation can be written as:



In this reaction, h⁺ and e⁻ are powerful oxidizing and reducing agents, respectively. The oxidation (2) and reduction (3) reactions can be expressed as:



Where O₂⁻ is a superoxide anion. When organic compounds are chemically transformed by a PCO, it is the hydroxyl radical (OH[•]), derived from the oxidation of adsorbed water or adsorbed hydroxide ion (OH⁻), that is the dominant strong oxidant. Its net reaction with a VOC can be expressed as (Mo et al., 2009):



Some reactants will generate partial oxidation products (intermediates) which are relatively more harmful to people's health (Mo J, Zhang Y et al., 2009). The oxidation process sometimes stops along the way yielding aldehydes, ketones and organics acids (Mo et al., 2009). For example, formaldehyde is frequently quoted as one of the main intermediates (Ginestet et al., 2005; Auvinen J et al., 2008; Kolarik J et al., 2010).

Furthermore, the photocatalyst may potentially emit some nanoparticles of TiO₂ in the indoor air. The TiO₂ dust, when inhaled, has been classified as possibly carcinogenic to humans (Group 2B) WHO (2010). The size of these nanoparticles may vary from 10 to 50nm INRS (2012).

A lot of studies use the PCO in a laboratory test chamber. Their volumes are very small (often less than 1m³) and most of the time the tests are carried out at constant air temperature (e.g. 20°C) and relative humidity (e.g. 50%), coupled with a constant injection of one to five different gases able to represent, partially, the indoor air.

In this study, a PS was developed embedding 4 layers with a total thickness of 5.5cm: an adhesive layer (0.3cm), a thermal insulation layer (3cm), a thermal storage layer (2cm), and a photocatalytic layer (0.2cm, directly in contact with the IA). This photocatalyst contained 5% of TiO₂ doped with carbon. Consequently, only 2.32 eV has to be transferred into this layer instead of 3.23 eV for the pure anatase. This study focuses only on the PCO impact on the indoor air quality of a room equipped with the PS (TR) and without the PS (RR).

2 METHODOLOGIES

2.1 Location of the tests

The tests were carried out in two rooms (the test room -TR- and the reference room -RR-) of an experimental test house located on the INCAS platform of the French National Institute of Solar Energy (INES). To compare the TR and the RR, each room was covered with an identical sarcophagus (SG) on the walls and the ceiling. This SG was made of plasterboard and was covered with 2 layers of white paint. After the SG installation, the TR and the RR had the same volume $3.62 \times 3.10 \times 2.34 \text{ m}^3$ and identical building materials, insulation, and paint. The rooms were south facing and they were juxtaposed on the first floor as shown in Figure 1.

To understand the PCO impact on the indoor air, the TR was equipped with the passive system (PS) and the RR was without the PS. No furniture was added in the TR and the RR. There was no air exchange rate to avoid new pollutants entering from the outside, and the doors and the windows remained closed. The sources of pollution mainly came from the PS in the TR and from the SG in the RR. The floors of the TR and the RR were covered with identical linoleum 4 years ago.

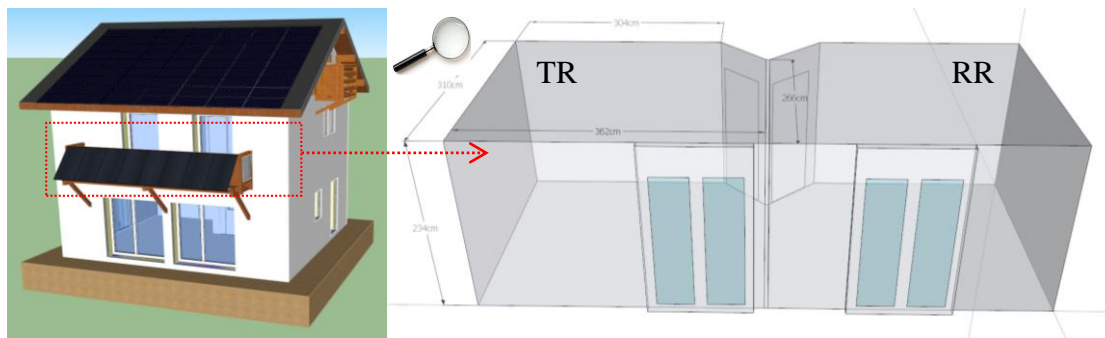


Figure 1. From the left to the right: illustration of the experimental test house, and localization of the test room (TR) and the reference room (RR)

2.2 Measurement campaigns

Four measurement campaigns were carried out to quantify the impact of the PS on the IA.

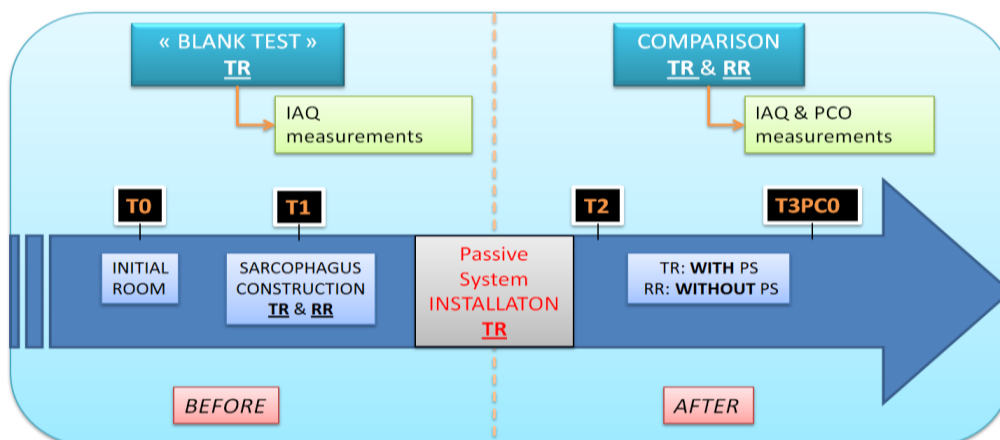


Figure 2. Four different steps, from January to May, to quantify the impact of the PS on the indoor air

The steps T0 and T1 were an “IAQ blank test” focused only on the TR. T0 corresponded to the room in its original state whereas T1 was equipped with the SG, see Figure 2. The parameters monitored and their positioning are indicated in the Table 1.

The step T1 monitored, directly after the installation of the SG, the same parameters as the previous step T0. In addition, the HCHO concentration was monitored to assess the SG emission and to compare this result with the HCHO concentration coming from the PS in the next step T2.

The step T2 was done right after the PS installation both in the TR and the RR. To highlight the PCO efficiency (T2) and to compare the results with the RR and the previous steps (T0 and T1), the tests were carried out without interference: no occupants, no intrusions, no furniture, doors and windows closed, mechanical ventilation system (MVS) was off, and the roller blind remained open.

In the final step T3PCO, the difference with T2 came from the use of specific actuators to modify the indoor environment modifying the behaviour of the PCO. The TR and the RR were equipped with identical resistances to make a ramp of temperature, visible lamps and UVA lamps (only in the TR) to activate the PCO, fans to mix the IA and improve the contact time with the TiO₂, roller blinds opened or closed to show the impact of the natural light on the PCO, and finally the MVS turned ‘on’ coupled with the opening of the door or the window to compare the PCO efficiency and the ventilation on the IAQ.

2.3 Parameters monitored

For the main parameters (Table 1), the monitoring was principally focused on the TR where the passive system was installed. To highlight the PCO effects, the measurements were made before and after the PS installation, and in comparison with the reference room (RR) when possible. The air temperature (Ta) and the relative humidity (RH) were monitored at each step in the TR, then in the two rooms after the PS installation. These parameters are some key factors for the PCO efficiency as well as the pollutant concentration, the type of photocatalyst and its quantity, the type of lighting and so on (Mo et al., 2009; Juan et al., 2003). As the photocatalyst layer should remove the VOCs and give off some carbon dioxide (CO₂), the total volatile organic compounds (TVOC) and the CO₂ were monitored. The formaldehyde (HCHO) was also measured as one possible intermediate as well as the number and the diameter of the nanoparticles (NP) to highlight a possible release of TiO₂ in the indoor air. The TVOC, CO₂, HCHO, NP were monitored before and after the PS installation and compared with the RR when it was possible (for more details, cf. Table 1).

Table 1. Information about the sensors used

| Parameters | Sensor model | Type of sampling | Rooms monitored | Steps | Probe positioning | Duration (Days) | Time step |
|---------------------------|--------------------------------|---|-------------------|-------------------|-------------------|-----------------|-----------|
| CO ₂ (ppm) | VAISALA MI70 & GMP70 | Continuous | TR | T0/T1 T2/T3PCO | CR H: 125cm | ≥ 7 | 5 min |
| NP (p/l & Ø:nm) | GRIMM NanoCheck model 1.365 | Continuous | TR | T0/T1 T2/T3PCO | CR H: 125cm | ≥ 7 | 10 s |
| HCHO (ppb) | ETHERA Profil'air® Dynamic Kit | Integrated measurement (every 2h from 9am to 5pm) | TR | T1/T2 T3PCO | CR H: 125cm | ≥ 5 | 4 S/D |
| TVOC (mg/m ³) | INNOVA 1412i & 1303 | Continuous | TR & RR | T0/T1 T2/T3PCO | CR H: 125cm | ≥ 7 | ≤ 5 min |
| Ta (°C) RH (%) | VAISALA HMP 110 | Continuous | TR → TR & RR → | T0/T1 T2/T3PCO | CR H: 125cm | ≥ 7 | 1 min |

CR: Centre of the room; S/D: sample per day; p/l: Number of nanoparticles per litre; Ø: diameter of nanoparticles (nm).

3 RESULTS AND DISCUSSION

The Table 2 shows a normal carbon dioxide concentration which fluctuated, for T0 and T1, around the ambient CO₂ concentration of 400ppm ASHRAE (2007). For T2 and T3PCO, the CO₂ concentration was very low (\pm 40ppm) and \approx 10 times less than the ambient CO₂ concentration (Cf. Table 2). These results didn't come from a measurement mistake or a CO₂ stratification because additional measurements were made to invalidate these hypotheses. This low concentration was due to a sink effect between the CO₂ and the calcium hydroxide Ca(OH)₂ embedded in the PS to form calcium carbonate (CaCO₃) and water. The equation can be written as:



After the PS installation there was not a significant difference of air temperature between the TR and the RR. The main difference concerned the relative humidity parameter with a higher level in the TR (almost twice as high) than in the RR especially during the step T2. This high concentration in the TR came from the PS containing 80% of water in its structure. For the step T1, the sarcophagus multiplied the TVOC concentration by 7.5, inside the TR in comparison with T0 (cf. Table 2).

Table 2. Average values of all parameters monitored from the steps T0 to T3PCO

| Steps | | T0 | | SG C* | T1 | | PS C* | T2 | | T3PCO | |
|---------------------------|--------|----------------------|----|-----------------|----------------------|----|---------------|----------------------|------|---------------------|------|
| Date (year 2013) | | 28/01→04/02 | | 14/02 | 18/02→25/02 | | 06/03 | 18/03→26/03 | | 19/04→02/05 | |
| Rooms | | TR | RR | SG in TR and RR | TR | RR | PS only in TR | TR | RR | TR | RR |
| CO ₂ (ppm) | | 392 | / | | 440 | / | | 36 | / | 53 | / |
| TVOC (mg/m ³) | | 4.23 | / | | 30.6 | / | | 212.9 | 15.5 | 53.2 | 20.7 |
| HCHO (ppb) | | / | / | | 175.3 | / | | 22.9 | / | 137.6 | / |
| NP | p/l | 2.04x10 ⁶ | / | | 9.61x10 ⁵ | / | | 3.66x10 ⁶ | / | 7.2x10 ⁷ | / |
| | Ø (nm) | 47 | / | | 67 | / | | 45 | / | 25 | / |
| Ta (°C) | | 16.0 | / | | 20.6 | / | | 14.2 | 14.4 | 27.7 | 25.2 |
| RH (%) | | 36.6 | / | | 40.7 | / | | 87.3 | 52.2 | 64.1 | 43.4 |

SG: Sarcophagus; PS: Passive system; C*: Construction; p/l: Number of nanoparticles per litre;

Compared to the step T1, the HCHO concentration decreased and was reduced by a factor of 9 after the installation of the PS (step T2), whereas at the same time, the TVOC concentration increased strongly by a factor of 7.

The decrease of the HCHO concentration is likely due to the high RH inside the TR (around 87%, Table 2) because the formaldehyde has a good solubility in the water INRS (2011). The HCHO was probably dissolved in the adsorbed water or condensed water (Pei et al., 2011) on the windows. Furthermore, a high water vapour concentration saturates the photocatalyst surface (Mo et al., 2009; Wang et al., 2007; Juan et al., 2003; Gaya et al., 2008). An excessive water vapour competes with pollutants such as VOCs for an adsorption site on the photocatalyst, thus reducing the pollutant removal rate. This is the "competitive adsorption" between the water vapour and the pollutants (Zhong et al., 2010; Mo et al., 2009; Wang et al., 2007). This phenomenon could explain the high TVOC concentration for the step T2.

Compared to T2, the step T3PCO had a TVOC concentration divided by 4 whereas the HCHO concentration increased and was multiplied by 6. Even if the TVOC concentration decreased, the value was still high (>50mg/m³) compared with the RR (Table 2). The decrease

of the TVOC concentration can be explained by a long period between T2 and T3PCO (23 days), a natural decrease of the VOCs emissions in the time coming from the PS, and a lower RH (64%) in the TR limiting the “competitive adsorption” phenomenon.

3.1 Impact of the actuators on the PCO efficiency

At the beginning of T3PCO, the Figure 3 shows an increase of the TVOC concentration in the TR and the RR. The doors and the windows were just closed and the MVS was turned off. The previous days before T3PCO, the doors were opened and the MVS was turned on to dry out the room and reduce the RH.

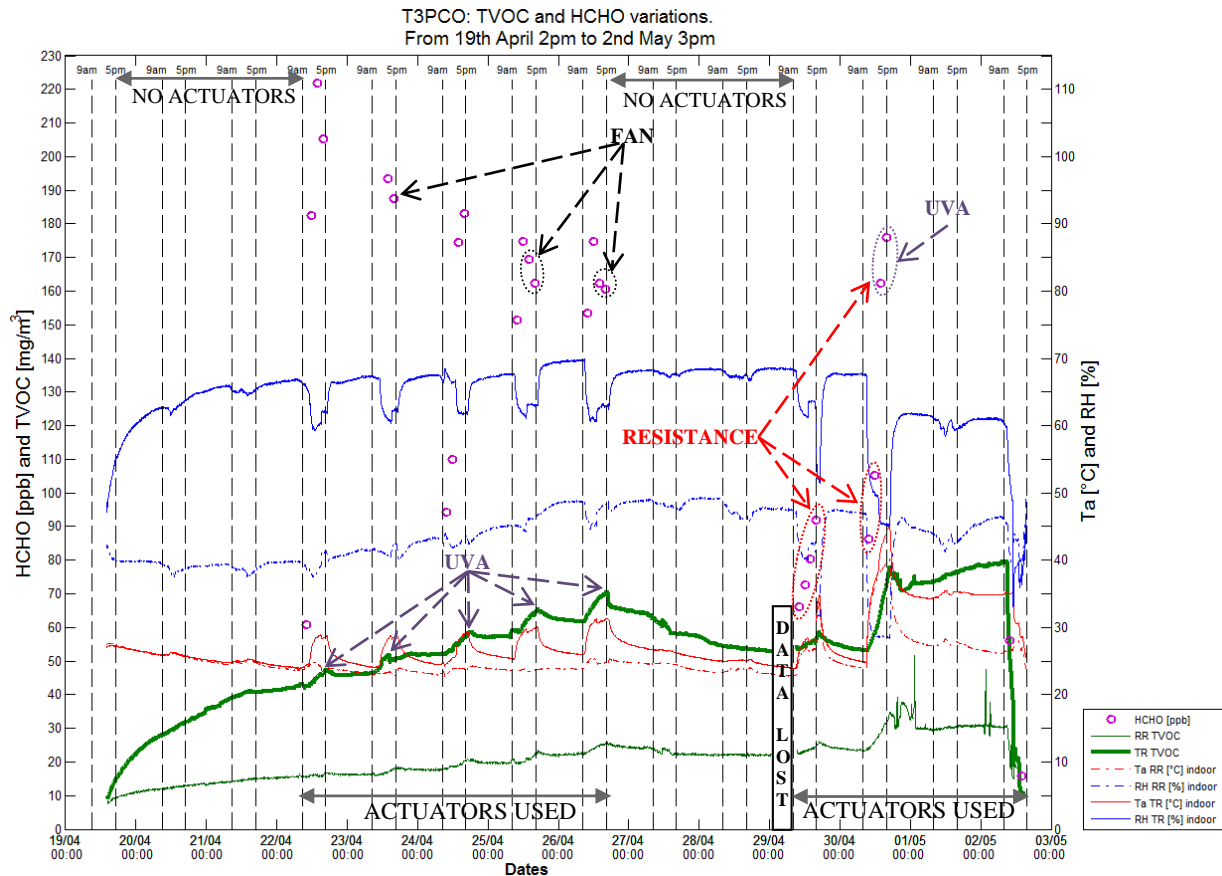


Figure 3. HCHO and TVOC concentrations for the step T3PCO

Every night, the Figure 3 shows a decrease or a stabilization of the TVOC and HCHO concentrations. Every night there was no heating system (Figure 3). Consequently the air temperature naturally decreased and an adsorption phenomenon of the pollutants occurred (Zhong et al., 2010).

Figure 3 shows the ramp of temperature from 9am to 1pm on the 30th April. It raised the TVOC concentration by +8mg/m³ and the HCHO concentration by +19.1ppb. In the afternoon the UVA lamps were added to the heating system. The impact on the TVOC concentration is significant (+16.9 mg/m³) as well as for the HCHO concentration (+89.9ppb). When the UVA lamps were turned on the TVOC increased as well as the HCHO (Auvinen et al., 2008; ADEME, 2013). The UVA activates the HCHO emission as an intermediate.

From 30th April 5:00pm to 2nd May 9:00am, a long test period was made with only the UVA lamps turned on to test the impact on the PCO. The results showed a ‘linear’ increase of TVOC. There was no PCO effect.

The fans coupled with the UVA lamps seem to stabilize or slightly reduce the HCHO emissions (Cf. 23rd, 25th, 26th April of the Figure 3). This is probably due to better air recirculation on the photocatalyst surface as well as a better contact time ADEME (2013). The last day (2nd May at 9am), the MVS was turned on for 2 hours in the TR and the RR, then the door was also added for 2 hours, as well as the windows for the following 2 hours. The TVOC and the HCHO concentrations were almost divided by 4 in 6 hours. At the end, the TVOC concentrations were equivalent and slightly inferior to 10mg/m³ for the TR and the RR.

3.2 Nanoparticles results and discussion

The bar graph shows (Figure 4) a lower number of NP coupled with a higher diameter than before the installation of the PS (steps T0 and T1). After the PS installation, the Figure 4 shows an increase of the number of NP coupled with a decrease of their diameter (Table 2). Under UVA radiation, the bar graph shows a huge increase of TiO₂ nanoparticles (the number of NP per litre was multiplied by 19.5 for T3PCO in comparison to T2). The reference OQAI (2012) speaks about an increase of TiO₂ nanoparticles <200nm under a UV radiation. To finish, the diameter of the NP measured in the step T3PCO (Ø: 25nm) tended toward the crystalline size of the TiO₂ used in the photocatalyst layer (Ø: 15nm for the step T3PCO).

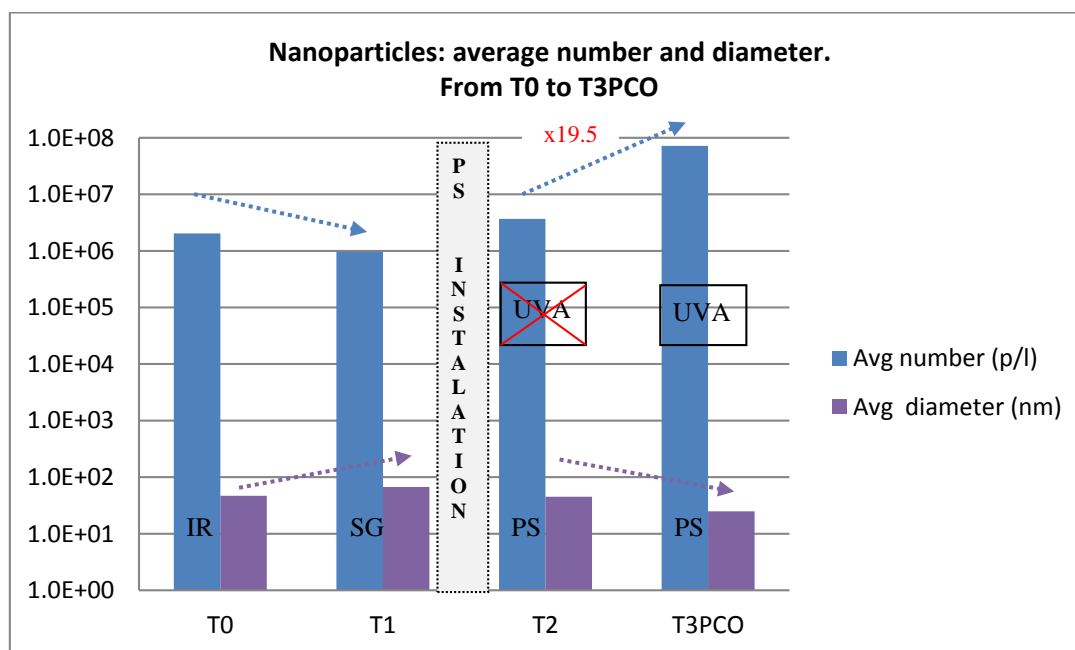


Figure 4. Nanoparticles measured in the TR, from the steps T0 to T3PCO (IR: Initial Room; SG: Sarcophagus; PS: Passive system)

4 CONCLUSIONS

In this study, the efficiency of the PS generated some disappointing results in a real indoor environment. This PS was embedded with 3 different layers plus a specific TiO₂ layer to improve the IAQ. The PS was applied onto the walls and the ceiling of the TR and was compared to a RR without anything added. There are several key factors to enhance the PCO efficiency: the temperature (Zhong et al., 2010; Mo et al., 2009), the water vapour concentration (Whang et al., 2007), the contaminant mixture (Ao et al., 2004), the quantity of photocatalyst substrate OQAI (2012), the amount of UVA lamps (Juan et al., 2003), etc.

For the step T2, immediately after the installation of the passive system, there was a high emission of VOCs in comparison to the RR and to the previous steps T1 and T0.

The high amount of water embedded in the PS (80%) increased the RH up to 90% in the TR, for the step T2. A high RH is responsible for a competitive adsorption between the water vapour and the pollutants onto the photocatalyst surface thus reducing the PCO process. This could explain the high TVOC concentration for the step T2, as well as the low HCHO concentration compared to T1. The HCHO is extremely soluble in water and there was probably a dissolution of this pollutant in the water vapour which was preferentially adsorbed by the photocatalyst surface rather than the TVOC pollutants.

For the step T3PCO, the results were not better with the use of actuators, especially the UVA-lamps. In the TR and the RR, there was a low UV light intensity because the window filtered the UV wavelengths. This lack of UV was compensated by the UVA lamps. When they were turned on for a long time (≈ 48 h), the UVA lamps did not enhance the PCO process but increased the TVOC and the HCHO emissions (intermediate).

Moreover, the results showed an increase of the air temperature due to the heating system and the UVA lamps. These 2 actuators were responsible for raising the TVOC and HCHO concentration. But the UVA raised the TVOC and the HCHO concentration more than the heating system. The combination of the opening of the door, window, and MVS showed a good improvement of the IAQ during the last day of the step T3PCO.

Finally, immediately after the PS installation (T2), there was an increase of NP and especially during the step T3PCO under UVA radiations. Without laboratory analysis, it is difficult to conclude formally about their origins even if their diameter (\varnothing : 25nm for T3PCO) tended toward the crystalline size of the TiO₂ nanoparticles used in the PS (\varnothing : 15nm).

The next step of further studies will consist of improving the efficiency of the PCO layer by dispersion of TiO₂ on a specific perlite substrate. This new PCO layer will be tested alone then with the PS.

ACKNOWLEDGEMENTS

The work described in this paper was supported by an FP7 research project funded by the European Commission: CETIEB (FP7 Grant Agreement No. 285623). I wish to thank my Work Package 5 partners and Jay Stuart.

REFERENCES

- Zhong L et al (2010) Modelling and physical interpretation of photocatalytic oxidation efficiency in indoor air applications. *Building and environment*, **45**, 2689–2697.
- Mo J et al (2009) Photocatalytic purification of volatile organic compounds in indoor air : A literature review. *Atmospheric Environment*, **43**, 2229–2246.
- Ginestet et al (2005) Development of a new photocatalytic oxidation air filter for aircraft cabin. *Indoor Air*, **15**, 326–334.
- Auvinen J et al (2008) The influence of photocatalytic interior paints on indoor air quality. *Atmospheric Environment*, **42**, 4101–4112.
- Mo J, Zhang Y et al (2009) Determination and risk assessment of by-products resulting from photocatalytic oxidation of toluene. *Applied Catalysis B: environmental*, **89**, 570–576.
- INRS (2012) Préconisation en matière de caractérisation des potentiels d'émission et d'exposition professionnelle aux aérosols lors d'opérations mettant en œuvre des nanomatériaux. *Institut National de Recherche et de Sécurité*, (HST ND2355-226-12).
- WHO (2010) World Health Organization, International Agency for Research on Cancer, Monographs on the Evaluation of carcinogenic Risks to Humans, Volume 93, Carbon black, Titanium Dioxide, and talc, Lyon France.

- Kolarik J, Wargocki P (2010) Can a photocatalytic air purifier be used to improve the perceived air quality indoors. *Indoor Air*, **20**, 255-262.
- Juan Z, Xudong Y (2003) Photocatalytic oxidation for indoor air purification: a literature review. *Building and Environment*, **38**, 645–654.
- ASHRAE (2007) Ventilation for acceptable indoor air quality, ASHRAE standard 62.1-2007, American Society of Heating, Refrigerating and Air–Conditioning Engineers, Inc., Atlanta, GA.
- Wang S et al (2007) Volatile organic compounds in indoor environment and photocatalytic oxidation: State of the art. *Environment International*, **33**, 694–705.
- Gaya UI, Abdullah AH (2008) Heterogeneous photocatalytic degradation of organic contaminants over titanium dioxide: A review of fundamentals, progress and problems. *Journal of Photochemistry and Photobiology C: Photochemistry Reviews*, **9**, 1–12.
- INRS (2011) Fiche toxicologique aldehydes formiques et solutions aqueuses, Institut National de Recherche et de Sécurité, FT7.
- Pei J, Jianshun S et al (2011) An experimental study of relative humidity effect on VOCs' effective diffusion coefficient and partition coefficient in a porous medium. *Chemical Engineering Journal*, **167**, 59–66.
- ADEME (2013) Fiche technique de l'ADEME, Epuration de l'air par photocatalyse. Agence de l'Environnement et de la Maitrise de l'Energie.
- OQAI (2012) Journée technique OQAI, RECUEIL DES RESUMES, L'épuration de l'air intérieur par les procédés photocatalytiques : efficacité et innocuité, Observatoire de la Qualité de l'Air Intérieur, Paris, France.
- Ao CH, Lee SC (2004) Photodegradation of formaldehyde by photocatalyst TiO₂: effects on the presences of NO, SO₂ and VOCs, *Applied Catalysis B: Environmental*, **54**, 41–50.